Journal of Neurorestoratology

Dovepress
open access to scientific and medical research

Open Access Full Text Article

ORIGINAL RESEARCH

Neurorestoratology evidence in an animal model with cervical spondylotic myelopathy

This article was published in the following Dove Press journal:
Journal of Neurorestoratology
17 January 2017
Number of times this article has been viewed

Xiang Li[1,2]
Guangsheng Li[1,3]
Keith Dip-Kei Luk[1]
Yong Hu[1–3]

[1]Department of Orthopaedics and Traumatology, The University of Hong Kong, Pokfulam, Hong Kong, [2]Shenzhen Key Laboratory for Innovative Technology in Orthopaedic Trauma, The University of Hong Kong-Shenzhen Hospital, Shenzhen, [3]Spinal Division, Department of Orthopaedics, Affiliated Hospital of Guangdong Medical University, Guangdong, People's Republic of China

Background: Cervical spondylotic myelopathy (CSM) is a chronic compression injury of the spinal cord, with potentially reversible conditions after surgical decompression, and a unique model of incomplete spinal cord injury. Several animal studies showed pathological changes of demyelination, axon loss and neuron apoptosis in rats with chronic spinal cord compression. However, there is a limited understanding of the neurological change in the spinal cord after surgical decompression. The aim of this study was to validate the neurorestoratology of myelopathic lesions in the spinal cord in a rat model.

Materials and methods: A total of 16 adult Sprague-Dawley rats were divided into four groups: sham control (group 1); CSM model with 4-week chronic compression (group 2), 2 weeks (group 3) and 4 weeks (group 4) after surgical decompression of CSM model. The compression and decompression were verified by magnetic resonance imaging (MRI) test. Neurological function was evaluated by Basso, Beattie, and Bresnahan (BBB) locomotor rating scale, ladder rung walking test and somatosensory-evoked potentials (SEPs). Neuropathological change was evaluated by histological examinations.

Results: MRI confirmed the compression of the cervical spinal cord as well as the reshaping of cord morphology after decompression. After decompression, significant changes of neurological function were observed in BBB scores ($p < 0.01$, $F = 10.52$), ladder rung walking test ($p < 0.05$, $F = 14.21$) and latencies ($p < 0.05$, $F = 5.76$) and amplitudes ($p < 0.05$, $F = 3.8$) of SEP. Neuronal degeneration was obvious in the ventral horn with gradual restoration. After decompression, the motor neuron number in the ventral horn did not show significant changes ($p > 0.05$). However, increasing trend of myelin area and staining intensity were observed in all columns of the white matter ($p < 0.05$) after decompression, especially in the compressed lateral column.

Conclusion: The established rat model is able to simulate histopathological characteristics of cervical myelopathy in human beings. The neuropathological change demonstrated that neurorestoratology in the myelopathic spinal cord would probably attribute to axonal remyelination of the white matter, but there would be an incapability of neuronal regeneration.

Keywords: neurorestoratology, surgical decompression, chronic spinal cord injury, animal model, cervical spondylotic myelopathy

Introduction

Cervical spondylotic myelopathy (CSM) is a chronic compression injury of the cervical spinal cord, leading to various neurological dysfunctions.[1–6] Surgical decompression could help to regain appreciable neurological function in many patients with CSM.[7–9] After decompression, the spinal canal would be enlarged and the strain and shear forces that applied on the cord would be removed, providing favorable anatomic microenvironment for the neurorestoratology.[10]

Correspondence: Yong Hu
Department of Orthopaedics and Traumatology, The University of Hong Kong, 12 Sandy Bay Road, Pokfulam, Hong Kong, People's Republic of China
Tel +852 2974 0359
Fax +852 2974 0335
Email yhud@hku.hk

submit your manuscript | www.dovepress.com
Dovepress
http://dx.doi.org/10.2147/JN.S123968

Previous studies stated that demyelination, axon damage and neuron death are the pathological changes in chronic compression-related myelopathy,[11] which was demonstrated by a lot of animal studies on compressive spinal cord injury.[11–14] Several recent animal studies on the CSM model presented histopathological consequences after chronic compression.[15–17] In the gray matter, the reduction in motor neuron number in the ventral horn as well as neuronal degeneration such as cavitation of cytoplasm and nuclear pyknosis and decrease in synapses are considered the initial pathomechanisms of CSM. In the white matter, disorganized fiber tract, decreased myelin sheath thickness, staining intensity or density and dissolved axons are considered the underlying neuropathological causes that attributed to subsequent neurological dysfunction. However, the gray matter is more vulnerable than the white matter, and the neuronal damage seems to be irreversible by the current available therapeutic strategy.

In acute spinal cord compression, remyelination of the demyelinated nerve fibers was observed by Gledhill et al[18] in a cat model. They concluded that the neurological deficit could be attributed to demyelination caused by acute cord compression and remyelination might contribute to functional recovery afterward.[18] In the condition of CSM, the remyelination of the axons may also be a critical mechanism accounting for neurorestoratology following surgical decompression.[19–22] Therefore, an attempt to preserve ascending and/or descending neural fiber tracts of the white matter seems to be attractive and promising. However, the exact role of remyelination in the recovery of postoperative CSM patients is also unclear.[23]

In this study, we produced chronic cervical cord compression on a rat model at C4/5 level and investigated the changes of neuropathology from chronic compressive spinal cord injury to surgical decompression. With this study, we hope to demonstrate the neurorestoratology in chronically compressed cervical spinal cord after surgical decompression.

Materials and methods

Materials

A total of 16 female adult Sprague-Dawley (SD) rats (220–250 g) were used in this study, provided by the Laboratory Animal Unit of the University of Hong Kong. These rats were evenly divided into four groups: sham control (group 1); CSM model with 4-week cervical cord compression (group 2); surgical decompression performed at 4 weeks after cervical cord compression and sacrificed at 2 weeks post decompression (D2W, group 3) and 4 weeks post decompression (D4W, group 4).

The rats were housed in cages with free access to water and food. All the animal-handling procedures of this study were performed according to the Guide for the Care and Use of Laboratory Animals. All animal experiments were approved by by the Committee on the Use of Live Animals in Teaching and Research of the University of Hong Kong.

Establishment of rat model

To create the compression injury to the cervical cord, a water-absorbing polymer[16] was made into a compression sheet in a standard size of 3 mm × 1 mm × 1 mm, which will expand its volume seven times within 2 hours by absorbing liquid in the spinal canal. This compression material did not elicit any tissue granulation or inflammatory reaction after implantation in the previous studies.[16]

The rats were operated on according to an established surgical protocol for implantation of water-absorbing materials.[16] After general anesthesia with intraperitoneal injection of 10% ketamine and 2% xylazine (Sigma Chemical Co., St. Louis, MO, USA), a skin incision was made to expose the C3–C7 laminae and the yellow ligament was removed between them through a posterior approach. A small space between the adjacent laminae near the facet at C5 level was opened and enlarged with natural flexion of the spine, while the underneath dura was carefully separated from the laminae. The polymer implant was carefully inserted into the right posterolateral side of the rat spinal canal at the planned compression level at C4/5. The polymer material gradually expanded to the maximum with seven times of its volume at 24 hours after implantation, and the pressure could maintain for 6 months. Then, the incision was carefully sutured after complete hemostasis. After recovery on a heating bed, the rats were returned to the cages and kept separately.

Surgical decompression of established rat model

For groups 3 and 4, surgical decompression was performed in animals 4 weeks after model establishment. The procedure was similar to the establishment of cervical cord compression. After exposing the laminae from C3 to C7 following anesthesia and incision, laminectomy was performed to remove the lamina from C3 to C5 on the right side. The expanded polymer sheet was taken out carefully. Then, the muscle and skin were sutured after complete hemostasis. After recovery on a heating bed, the rats were returned to the cages separately.

Magnetic resonance imaging (MRI)

All the MRI examinations were carried out using a 7T Bruker PharmaScan 70/16 scanner (Bruker, Karlsdorf-Neuthard, Germany). Anatomical MRI images revealed the morphological changes of the cervical spinal cord from compression to decompression. The animals were anesthetized by the inhalation of isoflurane and kept warm using a heating pad underneath. A surface coil was placed over the cervical spine to acquire magnetic resonance (MR) signals. Axial T2W images were acquired for each rat. The imaging parameters were as follows: time of echo (TE)/time of repetition (TR) = 11/4200 ms (T2W), slice thickness = 1 mm, inter-slice distance = 1.1 mm and the number of excitation (NEX) = 4.

Neurobehavioral evaluation

Basso, Beattie, and Bresnahan (BBB) locomotor rating scale[24] and ladder rung walking test[25] were used to evaluate the neurological function weekly after compression established by two different investigators separately using blinded method. The measurement of BBB rating scale ranges from complete paralysis (score 0) to normal locomotion (score 21). The ladder rung walking task could precisely evaluate the forelimb walking skill of the rat. The rats were put on a horizontal ladder with rungs and were managed to walk across from one side to another. The intervals of the rungs were 2 cm from each other. A video camera (HDR-CX290; Sony Inc., Tokyo, Japan) was used to capture the walking process. The speed of the recorded videos was slowed down by 10 times for analysis. Mistake of forepaw placement when walking on the rung ladder was observed, and the number of mistakes was recorded in every 10 steps. The walking task was repeated three times, and the average number was used to calculate the error rate.[25] The neurological evaluation was performed weekly after model establishment until sacrifice.

Somatosensory-evoked potential (SEP) evaluation

The sensory function of the cervical spinal cord was evaluated by SEPs with the protocol using SEP signal recording equipment (YRKJ-A2004; Zhuhai Yiruikeji Co, Ltd, Zhuhai, People's Republic of China).[15] The animals were evaluated under general anesthesia with intraperitoneal injection of 10% ketamine/2% xylazine (Kethalar, 1 mL:1 mL) (Sigma Chemical Co.). A constant current stimulator was used with a 4.1 Hz square wave and 0.1 ms in duration to stimulate the median nerve on the forepaw. The cortical SEP was recorded at the skull over the sensorimotor cortex (2 mm posterior and 2 mm lateral to bregma). The SEP response to the stimulation was recorded in the average of 100 trials. The latency delay and amplitude of the SEP signals were measured and recorded.

Histological evaluation

The animals were euthanized with overdose of 20% pentobarbital (200 mg/mL, intraperitoneal injection) at each time point. The rat was perfused by adjusting the perfusion height (110 cm H_2O) at the rate of 20 mL/min through the ascending aorta, followed by 10% buffered formalin. After perfusion, the cord was harvested, immersed in 10% formalin for 12 hours and embedded in paraffin. The cord was continuously sectioned by microtome with a thickness of 5 μm. The sections were stained by hematoxylin–eosin (H&E) and Luxol fast blue (LFB) and then analyzed with a light microscope imaging system (Nikon H600L Microscope, Tokyo, Japan). In the images with H&E staining, the neurons of the ventral horn on the compression side were manually counted in 400× microscopic fields. LFB was used to stain the myelin in the white matter of the spinal cord, and the blue color intensity indicates the myelin content. The loss of myelin content suggests demyelination in the neural fiber, and the regain of the content implicates remyelination. The area and intensity of the myelin were measured at ventral cord (VC), lateral cord (LC) and dorsal cord (DC) on the compression side with ten randomly placed regions of interest (ROI; 0.05×0.05 mm^2) using ImageJ (version 1.47v; National Institutes of Health, USA).

First, a scale was set globally to all images based on the primary scale bar marked in the raw image obtained from the microscopic system. Ten randomly placed ROI at VC, LC and DC regions on the compression side were added for measuring. Then, "area" and "integrated density" in the set measurement module were selected to measure the myelin area and myelin staining intensity, respectively, in blue color in the ROI. The abovementioned quantitative measurements were carried out by two different investigators using blinded method, and the average results were calculated.

Statistical analysis

The group differences between neurobehavior assessment, SEP and histological evaluation were analyzed by one-way analysis of variance (ANOVA) with Tukey's post hoc tests, with significance level at 5% ($p < 0.05$). All the statistical analyses were performed by using IBM SPSS version 15.0 software (IBM Corp., Armonk, NY, USA).

Results

MRI

MRI results verified the cervical cord compression due to expanding compression from water-absorbing polymer after

implantation and thereafter successful surgical decompression. After compression, the expanding material induced epidural space-occupying lesion and caused severe deformation of the gray matter and white matter in the DC–LC at C4/5 spinal level, while no evidence of spinal cord edema, hemorrhage, intramedullary cavity and glial scar was identified clearly (in comparison to intact cord Figure 1A, deformity of the compressed cord can be seen in Figure 1B). At D2W, spinal canal enlargement with a gradual restoration of the sunken cord could be seen in the compression side (Figure 1C). At the end of 4 weeks after decompression surgery, the cord almost reshaped to be an integral cord morphology and structure based on visible inspection during the animal was euthanized (Figure 1D).

Neurobehavioral and functional evaluation

The average BBB scores (Figure 2) and error rates of ladder rung walking test (Figure 3) were used to examine the motor function. The animals presented abnormality in forepaw position and tail falling after the establishment of spinal cord compression and significant differences in BBB scores among different groups or time points were found by ANOVA ($p < 0.01$, $F = 10.52$). BBB scores showed progressive recovery of motor function after decompression from 2 weeks to 4 weeks. In the ladder rung walking test, the error rates of forepaw placement were compared among all the groups with significant differences ($p < 0.05$, $F = 14.21$). The error rate of the compression group was significantly higher than the normal group, demonstrating the neurological dysfunction of the established rat model. Moreover, we compared the error rates of the decompression group with the compression group. The results showed that the error rate of the two decompression groups was significantly lower than the compression group ($p < 0.05$), suggesting neurological function recovery after decompression.

The results of SEP evaluation are shown in Figure 4. The latencies and amplitudes of the SEP signal in response to the stimulation on the compression side were compared among different groups. The results showed that there were significant differences in latencies ($p < 0.05$, $F = 5.76$) and amplitudes ($p < 0.05$, $F = 3.8$) among all the groups (Figure 4). The latency of the compression group was significantly delayed compared with the normal group ($p < 0.05$). Latencies had a trend to decrease with time after surgical decompression, with a significant decrease at 4 weeks after decompression ($p < 0.05$). The amplitude was found significantly increased at 4 weeks after decompression in comparison with the compression group ($p < 0.05$). The changes in both latency and amplitude of SEP implied the restoration of neurological function that was attributed to cord decompression.

Histological evaluation

The histological evaluation was used to validate neurorestoratology after surgical decompression (Figure 5A3, B3, C3, A4, B4 and C4). In H&E staining, integral butterfly shaped structure of the gray matter (Figure 5A1), rich cytoplasm of large motor neuron (Figure 5B1) and organized white matter were clearly identified in the sham control group (Figure 5C1). In the compressed group, evident sunken deformation caused by the expanded compressor were observed in the dorsal-lateral side of the cord (Figure 5A2), while the deformation was observed in agreement with MRI findings. No tissue edema was found at the compression side. The motor neurons were smaller in size and in long spindle shape in the compression group (Figure 5B2) compared with the sham control group. Neuronal degeneration was obvious in the ventral horn of the compression side of the cord, including the deformation of larger motor neurons, loss of cytoplasm, karyopyknosis of the nucleus and decreased neuronal synapse, especially in the compression side (Figure 5B2). Significant loss of large motor neurons in the ventral horn on the compression side (Figure 6) was found in the myelopathic cord ($p < 0.05$, $F = 7.82$), while the number of motor neurons did not increase after cord decompression ($p > 0.05$), which may imply incapable or limited regeneration potential of neurons.

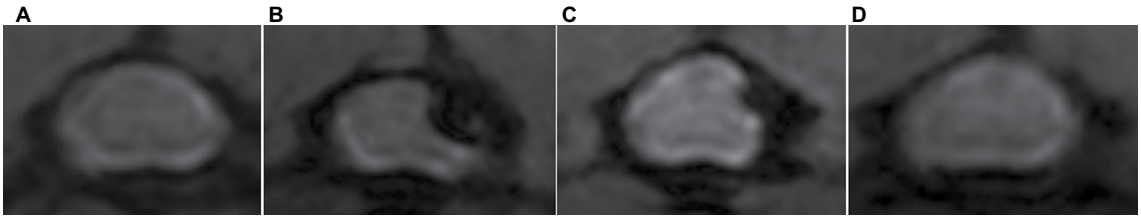

Figure 1 Cord compression and decompression verified by MRI detection.
Notes: T2W image before compression (**A**), after compression (**B**), 2 weeks after decompression (**C**) and 4 weeks after decompression (**D**).
Abbreviation: MRI, magnetic resonance imaging.

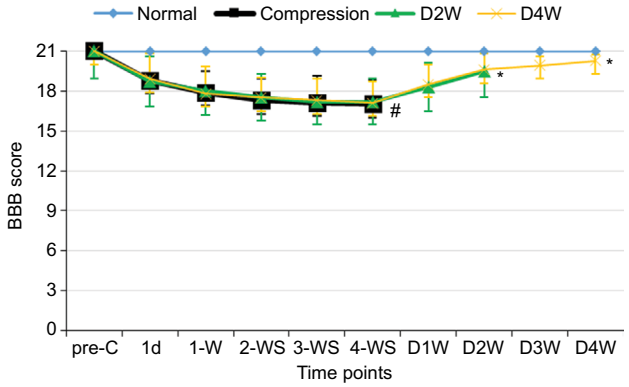

Figure 2 Motor function evaluation by BBB score.
Notes: Sham control group showed intact neurological function (blue base line). All of the model rats showed functional impairment, among the compression group (black line) at 4 weeks, D2W group (green line) and D4W group (orange line) before decompression. However, significant improvement was found ($p < 0.01$) after decompression and restoration of motor function evaluated by BBB score was evident in both the D2W and D4W groups, with 20.25 score reached in the D4W group at the final evaluation. These results suggested that neurological recovery can benefit from decompression strategy. #Different from the sham control group. *Different from the compression group ($p < 0.01$).
Abbreviations: BBB, Basso, Beattie, and Bresnahan; D1W, 1 week post decompression; D2W, 2 weeks post decompression; D3W, 3 weeks post decompression; D4W, 4 weeks post decompression; pre-C, before compression; 1d, 1 day; 1-W, 1 week; 2-WS, 2 weeks; 3-WS, 3 weeks; 4-WS, 4 weeks.

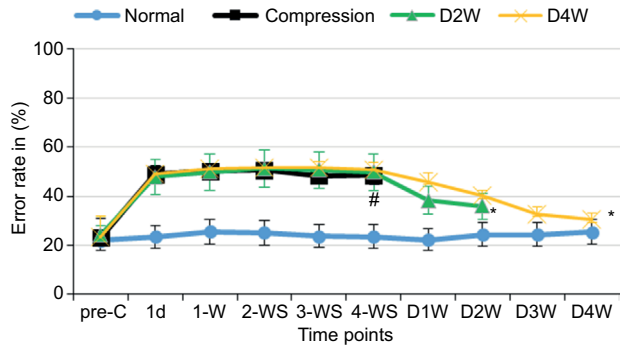

Figure 3 Motor function evaluation by ladder rung walking test.
Notes: Sham control group showed gentle fluctuation of error rate (blue line). After 4 weeks of compression, the error rate of ladder walking test increased significantly among the compression group (black line), D2W group (green line) and D4W group (orange line), which suggested the neurological dysfunction of established rat model. All of the model rats showed functional impairment after compression, among the compression group, D2W group (green line) and D4W group (orange line) at 4 weeks and before decompression. In comparison with the compression group, the error rate decreased significantly after decompression procedure at both 2 weeks and 4 weeks, demonstrating that neurological restoration resulted from surgical decompression. #Different from the sham control group. *Different from the compression group ($p < 0.05$).
Abbreviations: D1W, 1 week post decompression; D2W, 2 weeks post decompression; D3W, 3 weeks post decompression; D4W, 4 weeks post decompression; pre-C, before compression; 1d, 1 day; 1-W, 1 week; 2-WS, 2 weeks; 3-WS, 3 weeks; 4-WS, 4 weeks.

However, pathological restoratology was demonstrated after surgical decompression of the cord. Progressive cord reshaping and tissue reorganization in the decompression group from 2 weeks (Figure 5A3) to 4 weeks (Figure 5A4) indicated that surgical decompression contributed to morphological and structural reconstitution in the cord. Neuronal histopathology, such as similar regular morphology and rich or dense cytoplasm, can be restored partially (Figure 5B3 and B4), while atrophied nucleus and glial scar formation were observed in the D2W and D4W groups (Figure 5B3 and B4). In the white matter in H&E staining, sparse nerve fiber layers separated by vacuolated cords (Figure 5C2) due to chronic compression were gradually recovered in the D2W and D4W groups after surgical decompression (Figure 5C3 and C4).

In LFB staining, the myelin area and staining intensity were measured at VC, LC and DC of the compression side with ten randomly placed ROI. In the sham control group, organized neuropathological structure (Figure 7A1) and white matter fiber tracts were distinguishable clearly with dark blue staining and dense myelin sheath (Figure 7B1). In the 4-week cervical cord compression group (Figure 7A2), dissolved axons and sparse density of myelin sheath, and vacuolation change confirmed demyelinated degeneration in the white matter (Figure 7B2). Meanwhile, a significant difference between myelin staining area and intensity was found in VC, LC and DC in the compression group ($p < 0.05$, $F = 22.94$). In the D2W (Figure 7A3 and B3) and D4W groups (Figure 7A4 and B4), a continuous increase in myelin area appeared in all the columns of the white matter compared with the compression group (Figure 8), while the myelin area in VC, LC and DC of the white matter at 2 weeks after decompression was significantly smaller than the sham control group ($p < 0.05$). On the other hand, the staining intensity of all the other three groups was significantly lower (Figure 9) compared with the normal group in all the columns ($p < 0.05$). However, an increasing trend was noticed in the staining intensity from 2 weeks to 4 weeks after decompression in all the three columns ($p < 0.05$), indicating that axonal remyelination occurred after cord decompression.

Discussion

In this study, we successfully created an animal model with chronic cervical spinal cord compression in rats based on a previous study.[18] From the results of MRI, neurological function tests and histological examinations, we found that the cervical spinal cord was subjected to considerable posterolateral compression resulting from the polymer sheet implant. Neurophysiological changes were found in association with neuropathological changes, providing evidence of neurorestoratology in the myelopathic spinal cord.[26]

In this study, BBB scale and ladder rung walking test were employed for neurobehavioral assessment. In agreement, BBB scores and ladder rung walking test showed statistically

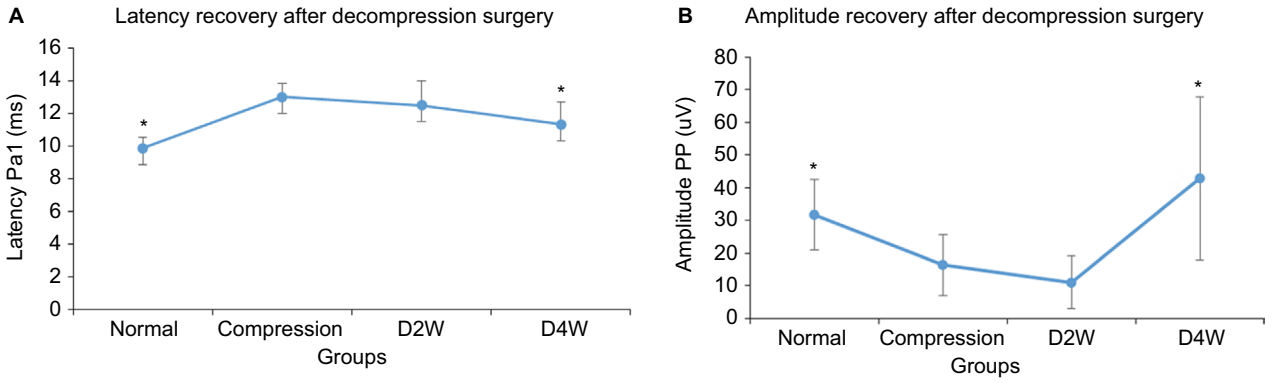

Figure 4 Sensory function evaluation by SEP test.
Notes: Latency delay was evident in the compression group ($p < 0.05$), while progressive recovery was demonstrated in the D2W and D4W groups after decompression (**A**). Amplitude of SEP decreased after compression, while significantly increased at 4 weeks after decompression (**B**). SEP test demonstrated neurological functional impairment after compression and restoration thereafter decompression. *Different from the compression group ($p < 0.05$).
Abbreviations: D2W, 2 weeks post decompression; D4W, 4 weeks post decompression; SEP, somatosensory-evoked potential; Pa1, peak 1; PP, peak-to-peak.

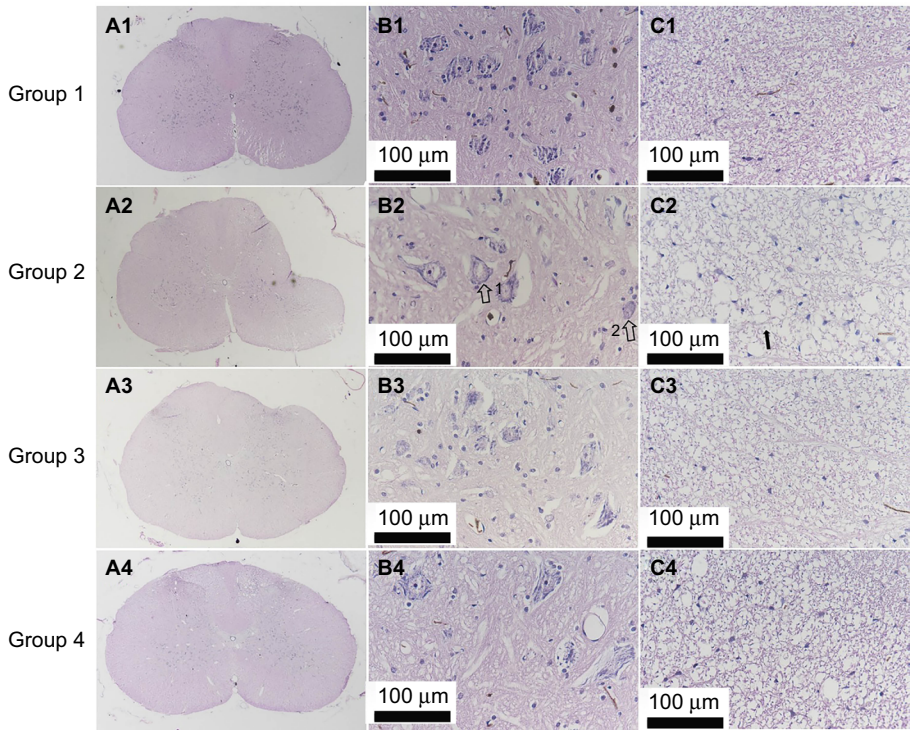

Figure 5 The histological results by H&E staining captured with 40× light microscope.
Notes: Group 1 (sham control): distinguishable structure (**A1**), large motor neuron with rich cytoplasm (**B1**) and dense neural fiber tissue of dorsal column (**C1**). Group 2 (CSM model with 4-week cervical cord compression): evident DC–LC compression and deformity (**A2**), neuron loss and loss of cytoplasm (hollow arrow 1), atrophied nucleus and glial scar formation (hollow arrow 2) (**B2**), sparse neural fiber with vacuolar degeneration of axon (black arrow) in the dorsal column (**C2**). Group 3 (2 weeks after decompression): cord shape restored with only minor cord deformity (**A3**), partial restoration of neuron cytoplasm (**B3**) and the recovery of sparse tissue of the dorsal column (**C3**). Group 4 (4 weeks after decompression), cord shape almost restored to normal condition (**A4**), neuronal degeneration was still identified (**B4**) and tissue restoration of dorsal column with reduced vacuolated cord (**C4**).
Abbreviations: CSM, cervical spondylotic myelopathy; DC, dorsal cord; H&E, hematoxylin–eosin; LC, lateral cord.

significant differences between the sham controls and cord compression as well as the two decompression groups. The results demonstrated that chronic compression induced motor function impairment in the model rats. The animal model used in this study was subject to chronic compression at the cervical spinal cord, which principally affected the sensory and motor functions of the forelimbs rather than hindlimbs.[27] Therefore, it may suggest the lower sensitivity of BBB scores in detecting the spinal cord dysfunction initiated by chronic compression. To the contrary, the ladder rung walking test was good at evaluating the precision of the forepaw placement while the rats were walking on a ladder with evenly distributed rungs. In this study, the neurobehavioral deficit of the compression group was well uncovered and the functional recovery was

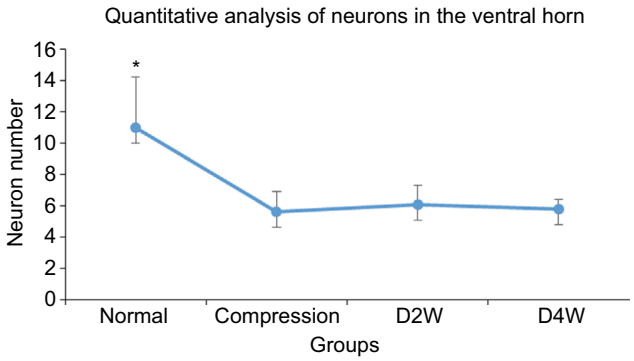

Figure 6 Quantitative analysis of large motor neuron.
Notes: The number of large motor neurons decreased significantly among the compression, D2W and D4W groups, while the number did not increase after surgical decompression compared with the compression group. *Different from the compression, D2W or D4W groups ($p < 0.05$).
Abbreviations: D2W, 2 weeks post decompression; D4W, 4 weeks post decompression.

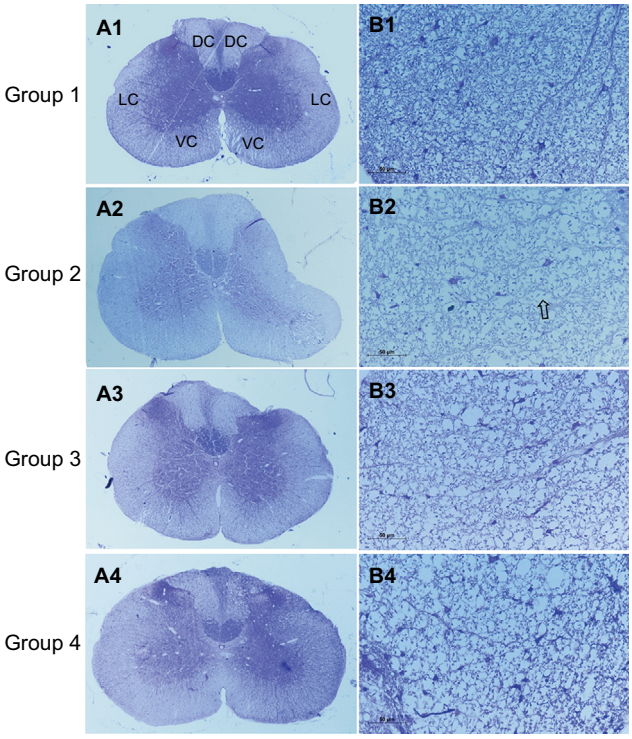

Figure 7 LFB staining showed myelination in the DC on the compression side captured with 400× light microscope.
Notes: Group 1 (sham control): identified butterfly shape and organized neuropathological structure (**A1**), and clearly recognized fiber tract with dense blue staining myelin (**B1**). Group 2 (4-week cervical cord compression): cord distortion and loss of dorsal–lateral white matter (**A2**) and decreased staining intensity with vacuolated change (**B2**, blank arrow). Group 3 (2 weeks after decompression): recovery of cord morphology (**A3**) and increased myelin staining area and intensity (**B3**). Group 4 (4 weeks after decompression), almost reconstitution of cord structural integrity (**A4**) and continuous restoration of vacuolated change and myelin staining (**B4**).
Abbreviations: DC, dorsal cord; LC, lateral cord; LFB, Luxol fast blue; VC, ventral cord.

statistically outlined in the two decompression groups. This suggested that the animal model used in this study could produce the long-term forelimb dysfunction resulting from the

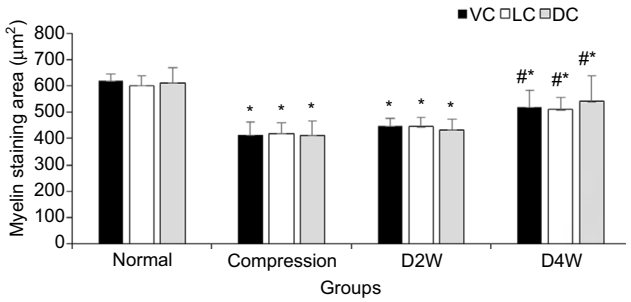

Figure 8 Analysis of myelin staining area at VC, LC and DC column in the white matter.
Notes: The results showed that myelin staining area decreased at all the three columns in the white matter in the compression group ($p < 0.05$). An increasing trend was demonstrated in the D2W and D4W groups after cord decompression, while such area was still small compared to that in the sham control group ($p < 0.05$), which suggested the partial remyelination of axon. *Significant different from the sham control group ($p < 0.05$). #Significant different from the compression group ($p < 0.05$).
Abbreviations: DC, dorsal cord; D2W, 2 weeks post decompression; D4W, 4 weeks post decompression; LC, lateral cord; VC, ventral cord.

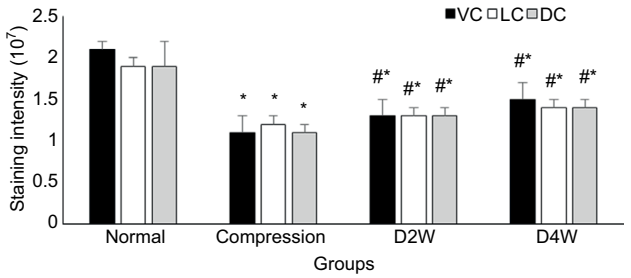

Figure 9 Analysis of myelin staining intensity at VC, LC and DC columns in the white matter.
Notes: The results showed that the myelin staining intensity decreased at all the three columns in the white matter in the compression group ($p < 0.05$). In comparison to the myelin staining intensity in compression group, there was a progressive significant increase in the staining intensity at all VC, LC and DC columns in the D2W and D4W groups after cord decompression, while the intensity was still lower than that in the sham control group ($p < 0.05$), implicating the partial remyelination of axon. *Significant different from the sham control group ($p < 0.05$). #Significant different from the compression group ($p < 0.05$).
Abbreviations: DC, dorsal cord; D2W, 2 weeks post decompression; D4W, 4 weeks post decompression; LC, lateral cord; VC, ventral cord.

chronic cervical cord compression, which was similar to the pathophysiological properties and natural history of CSM.[15,16]

SEP, which is used as an assessment of functional integrity of the sensory pathway, is used to measure the brain activity that generates from the stimulation of peripheral nerve, such as median nerve or posterior tibial nerve, through the spinal cord, and up to the cortex.[28,29] In our previous study, SEP measurements of latency and amplitude have been demonstrated to be able to indicate the ultrastructural impairment of the spinal cord in chronic compressive injury.[30] In this study, SEP evaluation further confirmed the result of neurobehavioral assessment by quantifying the anomaly of signal conduction in the somatosensory system. In the compression group, increased latency was detected compared with the sham control group, implying that substantial neural damage formed in the sensory tracts located at LC and DC. After decompression,

the latency presented a pattern of stepwise reduction with time. The signal amplitude had a trend to decrease after cord compression and increase after decompression even though it failed to reach statistical significance. Combining the results of the neurobehavioral and SEP evaluation, we verified the neurological decline in cord compression and functional recovery after surgical decompression.

In agreement, the MRI finding was compatible with histopathological change by H&E and LFB staining. The exact neural damage of cord tissue was revealed by histological investigation. Notably, the cord tissue including gray and white matter was highly squeezed on the compression side (Figure 5B), resulting in increased density of neurons and axons in the compressed regions. After decompression, the cord expanded and almost restored to its original oval shape.

As a result, no significant changes of the number of neurons were observed at the ventral horn after decompression. This did not provide us evidence of neuronal regeneration in chronic spinal cord compression. The reason for this result may be due to the short time of the recovery period, as we only observed at 2 weeks and 4 weeks after decompression. However, this finding was consistent with previous reports.[16,31] On the other hand, the myelin area and staining intensity were measured on the LFB staining slices, both of which were lower in the decompression group than the sham control and gradually increased with the time after decompression. The myelin area and staining intensity represented the status of myelination of the axons in the white matter. By observing the reduction in myelination in the two decompression groups, we may infer that the axonal demyelination took place in the condition of chronic spinal cord compression. In addition, the myelination continued to increase steadily with the time after surgical decompression, which was consistent with the results of the animal and human studies.[19–22] Therefore, it can be inferred from the abovementioned data that both neuronal dysfunction and demyelination of the white matter would contribute to neurological deficit, while neurorestoratology in chronic spinal cord compression would probably attribute to remyelination of the white matter tract;[32] thus, interventions to preserve or protect subsequent neural fiber damage or degeneration in the white matter seem more valuable than to rescue irreversible neuron death in CSM.[33] To date, although great efforts still need to be encouraged to promote breakthroughs in effective therapeutic strategy for CSM, this established model platform would bring bright prospects for practicing various kinds of neurorestorative strategies.[34,35]

However, although histopathological evidence of neurorestoratology was demonstrated after decompression procedure in this study, immunochemistry and molecular biological methods should be carried out to provide more detailed information on mechanism exploration in further research.

Conclusion

The established rat model by water-absorbing polymer has great advantages in exploring pathological changes of cervical myelopathy, as well as neurological and histopathological recovery after treatment. Neuropathological evidence demonstrated that neurorestoratology would probably attribute to axonal remyelination of the white matter or neural fiber tract after surgical decompression. Therefore, it would be more efficient to perform neurorestorative therapy strategy on the white matter to rescue neurological function.

Acknowledgments

This study was supported by the National Natural Science Foundation of China (81572193), General Research Fund of the University Grant Council of Hong Kong (767511M), Shenzhen Knowledge Innovation Program of Basic Research Items of Guangdong Province (JCYJ20150331142757393) and Natural Science Foundation of Guangdong Province, China (2016A030313679).

Disclosure

The authors report no conflicts of interest in this work.

References

1. Bilston LE, Thibault LE. The mechanical properties of the human cervical spinal cord in vitro. *Ann Biomed Eng*. 1996;24(1):67–74.
2. Breig A. Overstretching of and circumscribed pathological tension in the spinal cord – a basic cause of symptoms in cord disorders. *J Biomech*. 1970;3(1):7–9.
3. Breig A, Turnbull I, Hassler O. Effects of mechanical stresses on the spinal cord in cervical spondylosis. A study on fresh cadaver material. *J Neurosurg*. 1966;25(1):45–56.
4. Henderson FC, Geddes JF, Crockard HA. Neuropathology of the brainstem and spinal cord in end stage rheumatoid arthritis: implications for treatment. *Ann Rheum Dis*. 1993;52(9):629–637.
5. Smith CG. Changes in length and position of the segments of the spinal cord with changes in posture in the monkey. *Radiology*. 1956;66(2):259–266.
6. Henderson FC, Geddes JF, Vaccaro AR, Woodard E, Berry KJ, Benzel EC. Stretch-associated injury in cervical spondylotic myelopathy: new concept and review. *Neurosurgery*. 2005;56(5):1101–1113.
7. Matsuda Y, Shibata T, Oki S, Kawatani Y, Mashima N, Oishi H. Outcomes of surgical treatment for cervical myelopathy in patients more than 75 years of age. *Spine*. 1999;24(6):529–534.
8. Sampath P, Bendebba M, Davis JD, Ducker TB. Outcome of patients treated for cervical myelopathy. A prospective, multicenter study with independent clinical review. *Spine*. 2000;25(6):670–676.
9. Ebersold MJ, Pare MC, Quast LM. Surgical treatment for cervical spondylitic myelopathy. *J Neurosurg*. 1995;82(5):745–751.
10. Huang HY, Chen L. Neurorestorative process, law, and mechanisms. *J Neurorestoratol*. 2015;3:23–30.

11. Yamaura I, Yone K, Nakahara S, et al. Mechanism of destructive pathologic changes in the spinal cord under chronic mechanical compression. *Spine*. 2002;27(1):21–26.
12. Baba H, Maezawa Y, Imura S, Kawahara N, Nakahashi K, Tomita K. Quantitative analysis of the spinal cord motoneuron under chronic compression: an experimental observation in the mouse. *J Neurol*. 1996;243(2):109–116.
13. Crowe MJ, Bresnahan JC, Shuman SL, Masters JN, Beattie MS. Apoptosis and delayed degeneration after spinal cord injury in rats and monkeys. *Nat Med*. 1997;3(1):73–76.
14. Fehlings MG, Skaf G. A review of the pathophysiology of cervical spondylotic myelopathy with insights for potential novel mechanisms drawn from traumatic spinal cord injury. *Spine*. 1998;23(24):2730–2737.
15. Hu Y, Wen CY, Li TH, Cheung MM, Wu EX, Luk KD. Somatosensory-evoked potentials as an indicator for the extent of ultrastructural damage of the spinal cord after chronic compressive injuries in a rat model. *Clin Neurophysiol*. 2011;122(7):1440–1447.
16. Long HQ, Li GS, Lin EJ, et al. Is the speed of chronic compression an important factor for chronic spinal cord injury rat model? *Neurosci Lett*. 2013;545:75–80.
17. Karadimas SK, Moon ES, Yu WR, et al. A novel experimental model of cervical spondylotic myelopathy (CSM) to facilitate translational research. *Neurobiol Dis*. 2013;54:43–58.
18. Gledhill RF, Harrison BM, McDonald WI. Demyelination and remyelination after acute spinal cord compression. *Exp Neurol*. 1973;38(3):472–487.
19. Al-Mefty O, Harkey LH, Middleton TH, Smith RR, Fox JL. Myelopathic cervical spondylotic lesions demonstrated by magnetic resonance imaging. *J Neurosurg*. 1988;68(2):217–222.
20. Hashizume Y, Iljima S, Kishimoto H, Hirano A. Pencil-shaped softening of the spinal cord. Pathologic study in 12 autopsy cases. *Acta Neuropathol*. 1983;61(3–4):219–224.
21. Hashizume Y, Iijima S, Kishimoto H, Yanagi T. Pathology of spinal cord lesions caused by ossification of the posterior longitudinal ligament. *Acta Neuropathol*. 1984;63(2):123–130.
22. Alafifi T, Kern R, Fehlings M. Clinical and MRI predictors of outcome after surgical intervention for cervical spondylotic myelopathy. *J Neuroimaging*. 2007;17(4):315–322.
23. Beattie MS, Manley GT. Tight squeeze, slow burn: inflammation and the aetiology of cervical myelopathy. *Brain*. 2011;134(pt 5):1259–1261.
24. Basso DM, Beattie MS, Bresnahan JC. A sensitive and reliable locomotor rating scale for open field testing in rats. *J Neurotrauma*. 1995;12(1):1–21.
25. Metz GA, Whishaw IQ. The ladder rung walking task: a scoring system and its practical application. *J Vis Exp*. 2009;28:e1204.
26. Huang HY, Sharma HS. Neurorestoratology: one of the most promising new disciplines at the forefront of neuroscience and medicine. *J Neurorestoratol*. 2013;1:37–41.
27. Martinez M, Brezun JM, Bonnier L, Xerri C. A new rating scale for open-field evaluation of behavioral recovery after cervical spinal cord injury in rats. *J Neurotrauma*. 2009;26(7):1043–1053.
28. Seyal M, Emerson RG, Pedley TA. Spinal and early scalp-recorded components of the somatosensory evoked potential following stimulation of the posterior tibial nerve. *Electroencephalogr Clin Neurophysiol*. 1983;55(3):320–330.
29. Nakanishi T, Shimada Y, Sakuta M, Toyokura Y. The initial positive component of the scalp-recorded somatosensory evoked potential in normal subjects and in patients with neurological disorders. *Electroencephalogr Clin Neurophysiol*. 1978;45(1):26–34.
30. Hu Y, Ding Y, Ruan D, Wong YW, Cheung KM, Luk KD. Prognostic value of somatosensory-evoked potentials in the surgical management of cervical spondylotic myelopathy. *Spine*. 2008;33(10):E305–E310.
31. Johansson BB. Regeneration and plasticity in the brain and spinal cord. *J Cereb Blood Flow Metab*. 2007;27(8):1417–1430.
32. Ek CJ, Habgood MD, Dennis R, et al. Pathological changes in the white matter after spinal contusion injury in the rat. *PLoS One*. 2012;7(8):e43484.
33. Andrews RJ, Quintana L. Full spectrum neurorestoratology: enhancing neuroresponse to disasters. *J Neurorestoratol*. 2014;2:95–106.
34. Grecco LLS, Michel S, Castillo-Saavedra L, Mourdoukoutas A, Bikson M, Felipe Fregni F. Transcutaneous spinal stimulation as a therapeutic strategy for spinal cord injury: state of the art. *J Neurorestoratol*. 2015;3:73–82.
35. Enomoto M. Therapeutic effects of neurotrophic factors in experimental spinal cord injury models. *J Neurorestoratol*. 2016;4:15–22.